

Phase-Contrast Clinical Breast CT: Optimization of Imaging Setups and Reconstruction Workflows

Giuliana Tromba¹✉, Serena Pacilè^{1,2}, Yakov I. Nesterets³, Francesco Brun^{1,2}, Christian Dullin⁴, Diego Dreossi¹, Sheridan C. Mayo³, Andrew W. Stevenson^{3,5}, Konstantin M. Pavlov^{6,7}, Markus J. Kitchen⁷, Darren Thompson^{4,6}, Jeremy M.C. Brown⁷, Darren Lockie⁸, Maura Tonutti⁹, Fulvio Stacul⁹, Fabrizio Zanconati¹⁰, Agostino Accardo², and T.E. Gureyev^{3,6,7,11}

¹ Elettra - Sincrotrone Trieste, Basovizza (Trieste), Italy
giuliana.tromba@elettra.eu

² Department of Engineering and Architecture, University of Trieste, Trieste, Italy

³ Commonwealth Scientific and Industrial Research Organisation, Melbourne, Australia

⁴ Department of Diagnostic and Interventional Radiology, University Hospital Göttingen, Göttingen, Germany

⁵ Australian Synchrotron, Melbourne, Australia

⁶ School of Science and Technology, University of New England, Armidale, Australia

⁷ School of Physics and Astronomy, Monash University, Melbourne, Australia

⁸ Maroondah Breast Screen, Melbourne, Australia

⁹ Department of Radiology, AOU - Trieste Hospital, Trieste, Italy

¹⁰ Department of Medical Science-Unit of Pathology, University of Trieste, Trieste, Italy

¹¹ ARC Centre of Excellence in Advanced Molecular Imaging, School of Physics, University of Melbourne, Parkville, Australia

Abstract. We present the outcomes of combined feasibility studies carried out at Elettra and Australian Synchrotron to evaluate novel protocols for three-dimensional (3D) mammographic phase contrast imaging. A custom designed plastic phantom and some tissue samples have been studied at diverse resolution scales and experimental conditions. Several computed tomography (CT) reconstruction algorithms with different pre-processing and post-processing steps have been considered. Special attention was paid to the effect of phase retrieval on the diagnostic value of the reconstructed images. The images were quantitatively evaluated using objective quality indices in comparison with subjective assessments performed by three experienced radiologists and one pathologist.

We show that the propagation-based phase-contrast imaging (PBI) leads to substantial improvement to the contrast-to-noise and to the intrinsic quality of the reconstructed CT images compared with conventional techniques as well as to an important reduction of the delivered doses, thus opening the way to clinical implementations.

Keywords: X-rays · Phase contrast · Computed tomography · Mammography · Synchrotron radiation · Breast CT

1 Introduction

In the current medical practice, two-dimensional (2D) X-ray mammography is the main examination for the diagnosis of breast cancer. Despite the great advances due to the introduction of more sensitive detectors and novel X-ray generators, the technique still produces a relatively high percentage of both false-positive and false-negative results [1].

The recently implemented digital tomosynthesis opened new perspectives for its ability to produce multiple 2D slices through the breast and reduces the camouflaging effect due to overlap of different tissue layers that takes place in projection X-ray imaging [2, 3]. However, the most attractive 3D approach remains computed tomography (CT). Breast CT has the important advantage to reduce the physical discomfort experienced by patients due to the painful compression of the breast in conventional mammography [4, 5] and to give a real 3D representation of the breast characteristics.

A few dedicated breast CT prototypes are in clinical use worldwide [6, 7] with very promising results. Similarly to conventional radiology, the main limit in this approach is the low absorption contrast between normal (fibrous) and abnormal tissue.

Phase-contrast techniques can have an important role in this framework. Feasibility studies [8] already showed the effectiveness of analyser-based CT (AB-CT) in the improved detection of tumours with a smaller radiation dose, compared to current clinical mammography. At the same time, recent studies [9–15] have shown that, alternative X-ray phase-contrast imaging methods, such as the propagation-based phase-contrast tomography (PB-CT), can deliver outcomes comparable to AB-CT in regards to image quality and dose, while being potentially simpler and cheaper to implement.

The aim of this work is to provide a path to clinical implementation of low-dose high-quality 3D mammographic imaging, which will result in improved breast cancer diagnosis, substantial reductions in radiation dose and removal of patient pain.

2 Materials and Methods

2.1 Experiments at the Australian Synchrotron

We have conducted in-line (propagation-based) phase-contrast CT imaging experiments [14] at the Imaging and Medical beamline (IMBL) of the Australian Synchrotron [16]. The detector used was a Hamamatsu CMOS Flat Panel Sensor C9252DK-14, utilised in partial scan mode, with the pixel size $100\ \mu\text{m} \times 100\ \mu\text{m}$, 1174×99 pixels ($H \times V$) field of view and 12-bit output. The detector has a CsI scintillator directly deposited on a 2D photodiode array.

A specially designed and fabricated phantom was used in this experiment. The phantom consisted of a cylindrical block made of polycarbonate, with the diameter of 10 cm and the height of 2 cm, having eight irregularly located cylindrical holes of 1 cm diameter, each filled with different substances: glycerol, CaCl_2 1 M, ethanol 35 v%, paraffin oil, water, fatty ham, meaty ham and fibrous ham. The sample was imaged with

monochromatic X-rays at three energies: 38 keV, 45 keV and 50 keV. The sample rotation-axis to detector distance (sample-to-detector distance, for short), R_2 , was set to one of four values including 27 cm, 1 m, 2 m and 5 m.

CT data analysis (including pre-processing of data, CT reconstruction and optional post-processing) was carried out using X-TRACT software [17]. It is well acknowledged [11] that phase retrieval using an algorithm based on the homogeneous transport of intensity equation (TIE-HOM) [18] results, in general, in reduced noise in reconstructed CT slices while preserving the sharpness of the edges when used with a proper regularization (δ/β) parameter. We applied the TIE-HOM algorithm to projection data sets and subsequently carried out FBP CT reconstruction. In order to restrict the absorbed dose to values currently accepted for standard mammographic screening, we restricted the number of projections to 361 over 180° . The mean glandular doses (MGDs), D , per complete CT scans, were between 4.7 mGy and 10.8 mGy, depending on the imaging parameters.

2.2 Experiments at Elettra

In-line phase-contrast CT imaging experiments [13] have been carried out also at the SYRMEP imaging beamline of the Elettra synchrotron light source [19]. The detector used for low dose scans was a Dalsa Argus CCD TDI sensor with a pixel size of $27\ \mu\text{m}$ and a maximum X-ray resolution up to 15 lp/mm. The detector used for the high resolution scans was a water-cooled CCD camera by Photonic Science, model VHR, 4008×2672 full frame, used in 2×2 binning mode (resulting in pixel size of $9\ \mu\text{m}$), coupled to a gadolinium oxysulfide scintillator placed on a fiber optic taper.

A large tissue specimen excised during a surgical mastectomy was scanned at high and low statistics using the Dalsa detector at 32 keV with a sample-to detector distance of 18 cm and 2 m. A centimeter size tissue sample containing a small lesion was scanned at higher resolution (using the Photonic Science detector) at 20 keV with sample-to-detector distances of 4 cm (simulating absorption), 30, 100 and 166 cm.

Datasets have been reconstructed using the SYRMEP Tomo Project (STP) in-house developed software [20] using several different reconstruction algorithms such as: Filtered Back Projection (FBP) [21], Simultaneous Iterative Reconstruction Technique (SIRT) [22], Simultaneous Algebraic Reconstruction Technique (SART) [23], Conjugate Gradient Least Squares (CGLS) [22], Equally Sloped Tomography (EST) [24], Total Variation (TV) minimization [25] and an iterative FBP algorithm [26]. Like for the Australian experiment a phase retrieval (phr) algorithm was applied prior to the actual reconstruction by processing each projection independently, in accordance with the TIE-HOM algorithm [18]. For each of the above approaches images were reconstructed with and without application of phase retrieval pre-processing.

2.3 Quantitative Evaluation of the Images: Objectives Quality Indexes and Radiological Assessment

Reconstructed images for the mastectomy sample were quantitatively evaluated using several full-reference and no-reference image quality assessment indexes [27]. Full

references indexes require the definition of a certain ‘reference image’ that in our case is the one obtained by applying the FBP reconstruction algorithm to the high statistics scan using all available projections. The considered full reference indexes were: Mean Squared Error (MSE), Signal-to-Noise Ratio (SNR), Universal Quality Index (UQI) [28], Noise Quality Measure (NQM) [29] and Structural Similarity Index (SSIM) [27]. Apart from the MSE index, higher values of SNR, UQI, NQM and SSIM correspond to higher image quality.

The no-references indexes used were: the Contrast-to-Noise ratio (CNR), the Full Width Half Maximum (FWHM) and the dimensionless no-reference intrinsic quality characteristic Q_s which incorporates both the noise propagation and the spatial resolution properties of a linear system [12, 30]. Since the evaluation of FWHM requires a well-defined image edge, this index was evaluated by considering the images of the polycarbonate phantom sample and analyzing the line profiles at the interface between the background and one of the details [13].

CT scans of the mastectomy sample, carried out at clinical dose, were also assigned with subjective radiological scores provided by three experienced radiologists and one pathologist who expressed a blind opinion about the recognition of the lesion borders and their spiculations, the visibility of small connective residues included in the adipose tissue, the perceived contrast and spatial resolution. A global score was given from 0, for the worst case to 4, for the best image, i.e. the above defined ‘reference image’. On the basis of these scores, the images were then classified into three categories: no-diagnostic power (radiological score from 0 to 2), where the lesion characterization is difficult to be done; poor diagnostic power (radiological score higher than 2 to 3), i.e. it would be possible to diagnose the tumour but without an accurate evaluation of spiculations and/or connective residues existing in the tissue; and full diagnostic power (radiological score higher than 3), where all the relevant features are detectable and quantifiable.

3 Results

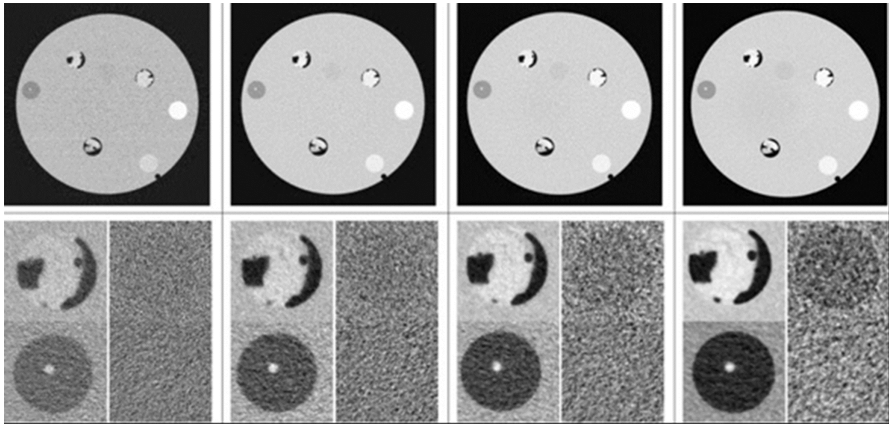
3.1 Outcomes from the IMBL Experiment

CT scans at the Australian Synchrotron were conducted at clinical doses and were focused to reveal the presence of phase effects, despite the large pixel size of the Hamamatsu detector widely used for conventional clinical imaging, and to evaluate the improvements of the image quality with respect to absorption images.

One reconstructed (using TIE-HOM phase retrieval with $\gamma = 1000$) CT slice from low photon statistics data (361 projections over 180°), corresponding to the X-ray energy of 38 keV, for four values of the sample-to-detector distance (0.27 m, 1 m, 2 m and 5 m) is shown in Fig. 1 together with its magnified fragments. Some quantitative image quality parameters, including the SNR per unit dose, $\text{SNR}/D^{1/2}$, and the intrinsic quality characteristic, $Q_s = \text{SNR}/D^{1/2}/(\text{Spatial resolution})$ [30], for four values of the propagation distance and using phase retrieval, are summarized in Table 1.

Table 1. Quality characteristics of CT slices reconstructed (using FBP) from phase-retrieved (using TIE-HOM).

Material	$R_2 = 0.27\text{m}^{\text{D}}$		$R_2 = 1\text{m}$		$R_2 = 2\text{m}$		$R_2 = 5\text{m}$	
	$\text{SNR} / D^{1/2}$ ($\text{mGy}^{-1/2}$)	$Q_s \times 10^4$ ($\mu\text{m}^2\text{mGy}^{-1/2}$)	$\text{SNR} / D^{1/2}$ ($\text{mGy}^{-1/2}$)	$Q_s \times 10^4$ ($\mu\text{m}^2\text{mGy}^{-1/2}$)	$\text{SNR} / D^{1/2}$ ($\text{mGy}^{-1/2}$)	$Q_s \times 10^4$ ($\mu\text{m}^2\text{mGy}^{-1/2}$)	$\text{SNR} / D^{1/2}$ ($\text{mGy}^{-1/2}$)	$Q_s \times 10^4$ ($\mu\text{m}^2\text{mGy}^{-1/2}$)
Polycarbonate	1.73 ± 0.02	122 ± 1	3.46 ± 0.03	217 ± 2	4.71 ± 0.04	283 ± 2	6.98 ± 0.06	402 ± 3
Glycerol	2.54 ± 0.02	179 ± 2	5.33 ± 0.04	333 ± 3	6.84 ± 0.06	406 ± 4	10.01 ± 0.09	576 ± 5
CaCl ₂ 1M	3.14 ± 0.03	222 ± 2	6.16 ± 0.05	383 ± 3	8.43 ± 0.07	504 ± 4	11.4 ± 0.1	651 ± 6
Ethanol 35v%	1.81 ± 0.02	128 ± 1	3.66 ± 0.03	232 ± 2	4.67 ± 0.04	280 ± 2	6.73 ± 0.06	385 ± 3
Paraffin oil	1.83 ± 0.02	127 ± 1	3.58 ± 0.03	221 ± 2	4.64 ± 0.04	274 ± 2	6.64 ± 0.06	374 ± 3
Water	2.23 ± 0.02	156 ± 1	4.43 ± 0.04	276 ± 2	5.88 ± 0.05	353 ± 3	8.18 ± 0.07	469 ± 4
Meaty ham	2.21 ± 0.02	157 ± 1	4.44 ± 0.04	289 ± 2	6.15 ± 0.05	387 ± 3	7.90 ± 0.07	463 ± 4

**Fig. 1.** Effect of phase retrieval on FBP CT reconstruction. The sample-to-detector distance, from left to right: 0.27 m, 1 m, 2 m and 5 m. Estimated Mean Glandular Doses (MGD) were 8.2 mGy, 8.2 mGy, 9.3 mGy and 10.8 mGy, respectively.

3.2 Outcomes from the Elettra Experiment

The first experiment conducted at Elettra was aimed at evaluating and optimizing the effects of phase contrast and phase retrieval in the detection of small malignant lesions in breast tissue specimens. For these purposes, high resolution scans (using the Photonic Science detector) have been performed at different propagation distances and the benefits of applying phase retrieval algorithm for the image quality have been evaluated in comparison with the absorption images. An example is shown in Fig. 2, where a representative slice of the tissue specimen obtained from the scan in absorption modality (a) is compared with the corresponding slice resulting from the phase-contrast scan obtained from phase-retrieved data; delivered doses were 4.8 and 5.8 Gy respectively.

In a quantitative images evaluation, a 20-fold improvement of the image quality-characteristic Q_s was found in the phase-retrieved image, which is equivalent to 400-fold reduction of X-ray dose at the same image quality. The second experiment carried

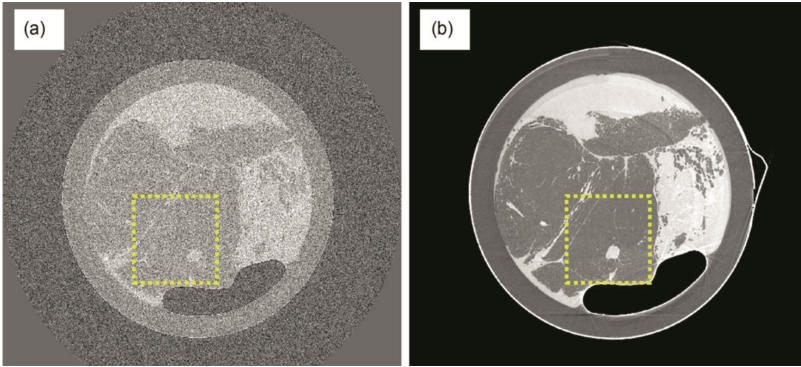


Fig. 2. Representative slice of the tissue specimen from absorption CT scan reconstructed with FBP (a) and phase contrast scan reconstructed with FBP after application of phase retrieval (b). The yellow box highlights a region with a suspect satellite lesion. (Color figure online)

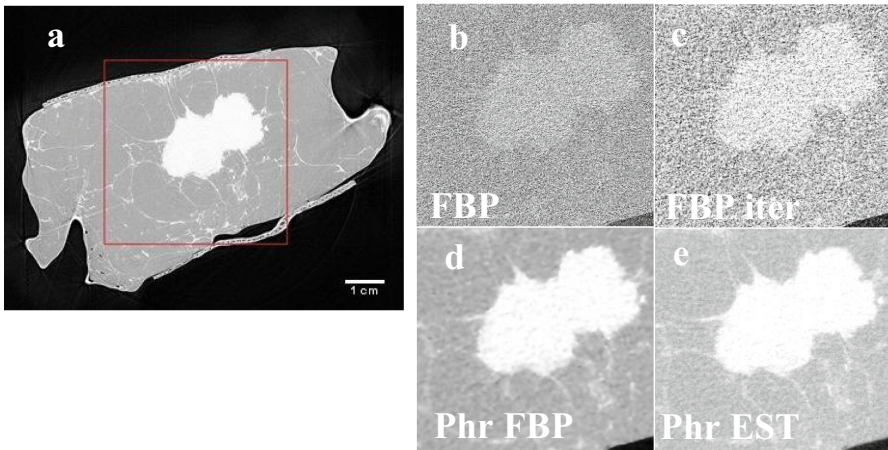


Fig. 3. Reference image for the mastectomy sample (a) and reconstructed images obtained with conventional FBP (b), Iterative FBP (c), Phr + Iterative FBP (d), Phr + EST algorithm (e).

out at Elettra was focused on low-dose CT scans using the Dalsa detector. The purpose of this experiment was to optimize the reconstruction workflow and perform a quantitative comparison of images obtained with different approaches, taking into account, with particular attention, the radiologist’s point of view. The considered reference image for the mastectomy sample, including a malignant lesion of about 3 cm with irregular edges, blurred margins and spicules, is shown in Fig. 3a.

This image was obtained at high dose, so that all the features are very well outlined. The red square indicates the region-of-interest (ROI) used for the image quality assessment. The low-dose CT scan, acquired at a MGD of about 1.5 mGy, was then considered,

several reconstruction approaches were applied and the respective ROIs were compared. Figure 3b, c show the slices obtained with conventional FBP and Iterative FBP algorithms, respectively, and were assigned by the radiologists to the ‘No diagnostic power’ class. Slices in Fig. 3d, e were obtained by applying the phase-retrieval pre-processing prior to the Iterative FBP and EST reconstruction respectively: both of them were evaluated in the ‘full diagnostic power’ class.

The correlation between the objective indexes and the radiological scores obtained for the same sample slice using different reconstruction workflows is shown in Fig. 4. In general, most of the image quality scores are in a good agreement with the radiological assessment, in particular the SSIM trend is the closest one.

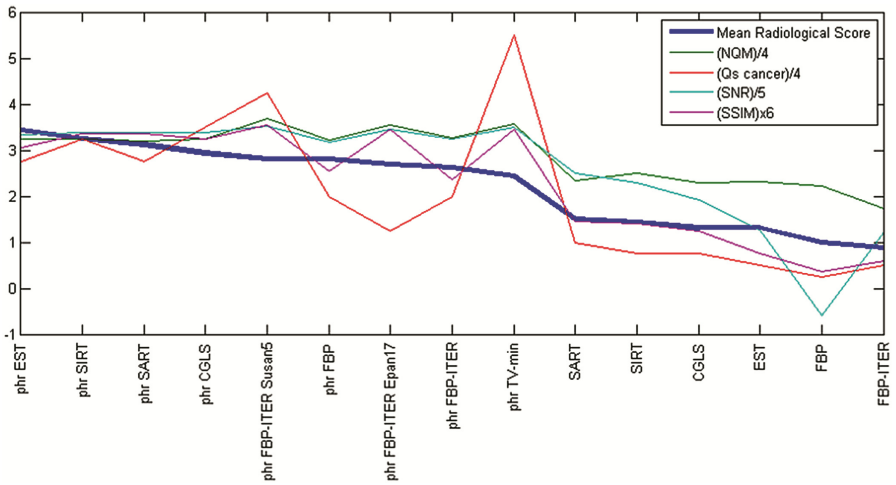


Fig. 4. Correlation between the radiological scores and various image quality indexes (Color figure online)

4 Discussion

Propagation-based phase-contrast CT with the application of phase retrieval using the TIE-HOM method with proper regularization (δ/β) parameter allows one to convert phase-contrast CT images into direct analogues of absorption CT images, while substantially increasing contrast-to-noise ratio without excessive image blurring. In fact, while a slight blurring effect induced by the application of phase retrieval can be perceived, the adoption of high resolution detectors (finer than the ones adopted in the nowadays clinical practice) and the significant benefits in terms of contrast and noise still supports the propagation-based CT approach. This conclusion is also validated by the qualitative evaluation performed by the radiologists. It was observed that the radiological assessment prefers, in all the cases, phase-retrieved images.

When comparing the performance of the same reconstruction algorithm with and without the application of phase retrieval (e.g. SIRT vs. phr SIRT), bigger values (indicating better quality) for the quality indexes like MSE, NQM and SNR were obtained, and similar trend was also found for the considered no-reference indexes CNR and Qs.

Strong improvement of CNR with phase retrieval was found particularly in the high resolution scans: for the small breast tissue specimen, a CNR value of up to 20 times bigger than in conventional CT was obtained at the same radiation dose.

At low dose, the application of phase retrieval makes the CT reconstruction much more effective. An example is shown in Fig. 3, where images reconstructed using FBP iterative algorithm without phase retrieval (Fig. 3c) are considered as having ‘no diagnostic power’, while the one obtained with the application of phase-retrieval pre-processing (Fig. 3d) has a high clinical quality (‘full diagnostic power’). By increasing the propagation distances to several meters, phase effects can be revealed even by a detector with relatively large pixel sizes (of the order of 100 μm), like in the case of Hamamatsu detector. As detectors with larger pixel sizes typically have higher detective quantum efficiency (DQE), compared to high-resolution X-ray detectors, the use of long propagation distances can become a valid possibility to reduce the radiation dose. It has to be pointed out that for this assumption an adequate spatial coherence of the source is required to avoid penumbral blurring: this is the case of synchrotron beamlines as well as last generation microfocus X-ray sources or compact sources.

5 Conclusions

The use of phase contrast and phase retrieval results in significant improvement in the quality of X-ray images of breast tissue. This has been demonstrated in the low-dose scans by evaluating several different quality indexes and considering the radiological assessment.

Low-dose phase-contrast CT images can be obtained with a conventional flat-panel detector having relatively large pixels if large propagation distances are implemented.

The outcomes of this study provide practical guidelines for the optimization of image processing workflows not only for synchrotron-based phase-contrast tomography but can be extended to new generator-based phase-contrast setups (gratings, coded aperture) or compact sources.

References

1. Pisano, E.D., Hendrick, R.E., Yaffe, M.J., Baum, J.K., Acharyya, S., Cormack, J.B., Hanna, L.A., Conant, E.F., Fajardo, L.L., Bassett, L.W., D’Orsi, C.J., Jong, R.A., Rebner, M., Tosteson, A.N.A., Gatsonis, C.A.: Diagnostic accuracy of digital versus film mammography: exploratory analysis of selected population subgroups in DMIST. *Radiology* **246**, 376–383 (2008)
2. Ciatto, S., Houssami, N., Bernardi, D., Caumo, F., Pellegrini, M., Brunelli, S., Tuttobene, P., Bricolo, P., Fantò, C., Valentini, M., Montemezzi, S., Macaskill, P.: Integration of 3D digital mammography with tomosynthesis for population breast-cancer screening (STORM): a prospective comparison study. *Lancet Oncol.* **14**, 583–589 (2013)

3. Pisano, E.D., Yaffe, M.J.: Breast cancer screening should tomosynthesis replace digital mammography? *JAMA* **311**(24), 2488–2489 (2014)
4. De Groot, J.E., Branderhorst, W., Grimbergen, C.A., den Heeten, G.J., Broeders, M.J.: Towards personalized compression in mammography: a comparison study between pressure- and force-standardization. *Eur. J. Radiol.* **84**(3), 384–391 (2015)
5. Papas, M.A., Klassen, A.C.: Pain and discomfort associated with mammography among urban low-income African-American women. *J. Community Health* **30**(4), 253–267 (2005)
6. Prionas, N.D., Lindfors, K.K., Ray, S., Huang, S.Y., Beckett, L.A., Monsky, W.L., Boone, J.M.: Contrast enhanced dedicated breast CT: initial clinical experience. *Radiology* **256**, 714–723 (2010)
7. O’Connell, A.M., Karellas, A., Vedantham, S.: The potential role of dedicated 3D breast CT as a diagnostic tool: review and early clinical examples. *Breast J.* **20**, 592–605 (2014)
8. Zhao, Y., Brun, E., Coan, P., Huang, Z., Sztrókay, A., Diemoz, P.C., Liebhardt, S., Mittone, A., Gasilov, S., Miao, J., Bravin, A.: High-resolution, low-dose phase contrast X-ray tomography for 3D diagnosis of human breast cancers. *Proc. Nat. Acad. Sci.* **109**(45), 18290–18294 (2012)
9. Diemoz, P.C., Bravin, A., Langer, M., Coan, P.: Analytical and experimental determination of signal-to-noise ratio and figure of merit in three phase-contrast imaging techniques. *Opt. Express* **20**, 27670–27690 (2012)
10. Gureyev, T., Mohammadi, S., Nesterets, Y., Dullin, C., Tromba, G.: Accuracy and precision of reconstruction of complex refractive index in near-field single-distance propagation-based phase-contrast tomography. *J. Appl. Phys.* **114**(14), 144906 (2013)
11. Nesterets, Y.I., Gureyev, T.E.: Noise propagation in X-ray phase-contrast imaging and computed tomography. *J. Phys. D Appl. Phys.* **47**(10), 105402 (2014)
12. Gureyev, T.E., Mayo, S.C., Nesterets, Y.I., Mohammadi, S., Lockie, D., Menk, R.H., Arfelli, F., Pavlov, K.M., Kitchen, M.J., Zanconati, F., Dullin, C., Tromba, G.: Investigation of the imaging quality of synchrotron-based phase-contrast mammographic tomography. *J. Phys. D Appl. Phys.* **47**, 365401 (365418 pp) (2014a)
13. Pacilè, S., Brun, F., Dullin, C., Nesterets, Y.I., Dreossi, D., Mohammadi, S., Tonutti, M., Stacul, F., Lockie, D., Zanconati, F., Accardo, A., Tromba, G., Gureyev, T.E.: Clinical application of low-dose phase contrast breast CT: methods for the optimization of the reconstruction workflow. *Biomed. Opt. Express* **6**, 3099–3112 (2015)
14. Nesterets, Y.I., Gureyev, T.E., Mayo, S.C., Stevenson, A.W., Thompson, D., Brown, J.M., Kitchen, M.J., Pavlov, K.M., Lockie, D., Brun, F., Tromba, G.: A feasibility study of X-ray phase-contrast mammographic tomography at the Imaging and Medical beamline of the Australian Synchrotron. *J. Synchrotron Radiat.* **22**, 1509–1523 (2015)
15. Longo, R., Arfelli, F., Bellazzini, R., Bottigli, U., Brez, A., Brun, F., Brunetti, A., Delogu, P., Di Lillo, F., Dreossi, D., Fanti, V., Fedon, C., Golosio, B., Lanconelli, N., Mettievier, G., Minuti, M., Oliva, P., Pinchera, M., Rigon, L., Russo, P., Sarno, A., Spandre, G., Tromba, G., Zanconati, Z.: Towards breast tomography with synchrotron radiation at Elettra: first images. *Phys. Med. Biol.* **61**, 1634–1649 (2016)
16. Stevenson, A.W., Mayo, S.C., Hausermann, D., Maksimenko, A., Garrett, R.F., Hall, C.J., Wilkins, S.W., Lewis, R.A., Myers, D.E.: First experiments on the Australian Synchrotron Imaging and Medical beamline, including investigations of the effective source size in respect of X-ray imaging. *J. Synchrotron Radiat.* **17**, 75–80 (2010)
17. Gureyev, T.E., Nesterets, Y., Ternovski, D., Thompson, D., Wilkins, S.W., Stevenson, A.W., Sakellariou, A., Taylor, J.A.: Toolbox for advanced X-ray image processing. *Proc. SPIE* **8141**, 1–14 (2011)

18. Paganin, D., Mayo, S.C., Gureyev, T.E., Miller, P.R., Wilkins, S.W.: “Simultaneous phase and amplitude extraction from a single defocused image of a homogeneous object. *J. Microsc.* **206**(1), 33–40 (2002)
19. Tromba, G., Longo, R., Abrami, A., Arfelli, F., Astolfo, A., Bregant, P., Brun, F., Casarin, K., Chenda, V., Dreossi, D., Hola, M., Kaiser, J., Mancini, L., Menk, R.H., Quai, E., Quaia, E., Rigon, L., Rokvic, T., Sodini, N., Sanabor, D., Schultke, E., Tonutti, M., Vascotto, A., Zanconati, F., Cova, M., Castelli, E.: The SYRMEP beamline of Elettra: clinical mammography and bio-medical applications. *AIP Conf. Proc.* **1266**, 18–23 (2010)
20. Brun, F., Pacilè, S., Accardo, A., Kourousias, G., Dreossi, D., Mancini, L., Pugliese, R.: Enhanced and flexible software tools for X-ray computed tomography at the Italian synchrotron radiation facility Elettra. *Fundamenta Informaticae* **141**(2–3), 233–243 (2015)
21. Kak, A.C., Slaney, M.: *Principles of Computerized Tomographic Imaging*. IEEE Press, New York (1988)
22. Van der Sluis, A., Van der Vorst, H.: SIRT- and CG-type methods for the iterative solution of sparse linear least-squares problems. *Linear Algebra Appl.* **130**, 257–303 (1990)
23. Gordon, R., Bender, R., Herman, G.: Algebraic reconstruction techniques (ART) for three-dimensional electron microscopy and X-ray photography. *J. Theor. Biol.* **29**, 471–476 (1970)
24. Miao, J., Frster, F., Levi, O.: Equally sloped tomography with oversampling reconstruction. *Phys. Rev. B* **72**, 052103 (2005)
25. Tang, J., Nett, B.E., Chen, G.: Performance comparison between total variation (TV)-based compressed sensing and statistical iterative reconstruction algorithms. *Phys. Med. Biol.* **54**, 5781–5804 (2009)
26. Myers, G.R., Thomas, C.D.L., Paganin, D.M., Gureyev, T.E., Clement, J.G.: A general few-projection method for tomographic reconstruction of samples consisting of several distinct materials. *Appl. Phys. Lett.* **96**, 021105 (2010)
27. Wang, Z., Bovik, A.C., Sheikh, H.R., Simoncelli, E.P.: Image quality assessment: from error visibility to structural similarity. *IEEE Trans. Image Process.* **13**, 600–612 (2004)
28. Wang, Z., Bovik, A.C.: A universal image quality index. *IEEE Signal Proc. Let.* **9**, 81–84 (2002)
29. Damera-Venkata, N., Kite, T.D., Geisler, W.S., Evans, B.L., Bovik, A.C.: Image quality assessment based on a degradation model. *IEEE Trans. Image Process.* **9**, 636–650 (2000)
30. Gureyev, T.E., Nesterets, Y.I., De Hoog, F., Schmalz, G., Mayo, S.C., Mohammadi, S., Tromba, G.: Duality between noise and spatial resolution in linear systems. *Opt. Express* **22**, 9087–9094 (2014)